Functional effects of a missense mutation in HERG associated with type 2 Long QT syndrome

Irene Amorós, Juan Jiménez-Jáimez, Luis Tercedor, Adriana Barana, Ricardo Gómez, Marta González de la Fuente, Pablo Dolz-Gaitón, Miguel Álvarez, Esther Martínez-Espín, José A. Lorente, Rafael Melgares, Juan Tamargo, Eva Delpón, Ricardo Caballero

PII: S1547-5271(10)01251-8
DOI: 10.1016/j.hrthm.2010.11.032
Reference: HRTHM 4200

To appear in: *Heart Rhythm*

Received date: 29 July 2010
Accepted date: 11 November 2010

Please cite this article as: Amorós, I., Jiménez-Jáimez, J., Tercedor, L., Barana, A., Gómez, R., de la Fuente, M.G., Dolz-Gaitón, P., Álvarez, M., Martínez-Espín, E., Lorente, J.A., Melgares, R., Tamargo, J., Delpón, E., Caballero, R., Functional effects of a missense mutation in HERG associated with type 2 Long QT syndrome, *Heart Rhythm* (2009), doi: 10.1016/j.hrthm.2010.11.032.

Functional effects of a missense mutation in HERG associated with type 2 Long QT syndrome

Irene Amorós BPharm,[1*] Juan Jiménez-Jáimez MD,[2*] Luis Tercedor MD,[2] Adriana Barana BSci,[1] Ricardo Gómez BPharm PhD,[1†] Marta González de la Fuente BPharm,[1] Pablo Dolz-Gaitón BSci,[1] Miguel Álvarez MD,[2] Esther Martínez-Espín PhD,[3] José A. Lorente MD PhD,[4] Rafael Melgares MD PhD,[2] Juan Tamargo MD PhD FESC,[1] Eva Delpón BPharm PhD,[1] Ricardo Caballero BPharm PhD.[1]

1: Department of Pharmacology. School of Medicine. Universidad Complutense. Madrid. Spain.
2: Arrhytmias Unit. Cardiology Department. Hospital Universitario Virgen de las Nieves. Granada Spain
3: LORGEN GP, S.L. BIC. Granada. Spain
4: Forensics and Legal Medicine Department & GENYO - Centro Pfizer. Universidad de Granada. Spain
*Contributed equally.

Short title: Functional effects of p.E637G Kv11.1 mutation.

Conflict of interest: The authors have declared that no conflict of interest exists.
Supported by Ministerio de Educación y Ciencia (SAF2008-04903), Ministerio de Sanidad y Consumo, Instituto de Salud Carlos III (Red HERACLES RD06/0009 and PI080665), Fundación LILLY, Centro Nacional de Investigaciones Cardiovasculares (CNIC-13), and Spanish Society of Cardiology grants.

† Corresponding author: Department of Pharmacology. School of Medicine. Universidad Complutense. 28040-Madrid. Spain. Tel: 34913941474. Fax: 34913941470 Email: ricardo.gomez@med.ucm.es

Abstract

Background: Long QT syndrome (LQTS) is characterized by a prolonged QT interval that can lead to severe ventricular arrhythmias (*torsades de pointes*) and sudden death. Congenital LQTS type 2 (LQT2) is due to loss-of-function mutations in the KCNH2 gene encoding Kv11.1 channels responsible for the rapid component of the delayed rectifier current.

Objective: To determine the functional properties of the LQT2-associated mutation p.E637G found in a Spanish family.

Methods: Wild-type (WT) and p.E637G Kv11.1 channels were transiently transfected in CHO cells and currents were recorded using the patch-clamp technique.

Results: p.E637G channels lost inward rectification and K^+ selectivity generating small but measurable slowly activating, non-inactivating currents. These important alterations were not corrected either by cotransfection with WT channels or by incubation at low temperatures or with pharmacological chaperones. As a consequence of its effects on channel gating, the mutation significantly reduced the outward repolarizing current during the action potential (AP), resulting in a marked lengthening of the duration of a simulated human ventricular AP.

Conclusion: We have identified and characterized a LQT2-associated mutation that through removal of C-type inactivation and reduction of K^+ selectivity causes the QT prolongation observed in the patients carrying the mutation. Moreover, the results obtained demonstrate the importance of the glutamic acid at position 637 for the inactivation process and K^+ selectivity of Kv11.1 channels.

Keywords: Long QT syndrome, Kv11.1 channels, missense mutation, patch-clamp, HERG

Abbreviations:

LQTS: long QT syndrome
I_{Kr}: rapid component of the delayed rectifier K^+ current
AP: action potential
WT: wild-type
CHO: Chinese Hamster ovary cells
I_{WT}: current generated by WT Kv11.1 channels
I_{E637G}: current generated by p.E637G Kv11.1 channels
$I_{WT/E637G}$: current generated by cells cotransfected with WT and p.E637G Kv11.1 channels
τ_{act}: time constant of activation
I-V: current-voltage
τ_f: fast time constant of deactivation
τ_s: slow time constant of deactivation
E_{rev}: reversal potential
V_h: midpoint of the activation/inactivation curve
k: slope of the activation/inactivation curve
$I_{Kv11.1}$: current generated by Kv11.1 channels

Introduction

Long QT syndrome (LQTS) is characterized by a prolonged QT interval that can be associated with syncope and sudden death due to *torsades de pointes* ventricular tachycardia and fibrillation.[1] Congenital LQTS type 2 (LQT2) is due to loss-of-function mutations in the KCNH2 gene (HERG).[1] KCNH2 encodes the pore-forming subunit of the channels (Kv11.1) that generate the rapid component of the delayed rectifier K^+ current (I_{Kr}), which is critical for action potential (AP) repolarization.[2] Approximately 450 LQT2-associated mutations are known so far and most of them are missense mutations.[2] The studies demonstrated that these mutations mostly affect protein folding, promote retention in the endoplasmic reticulum, or disrupt trafficking to the surface membrane.[2] Other mutations alter the gating of the channels by several mechanisms including enhance inactivation, acceleration of the deactivation rate, or shifting in the voltage dependence of channel inactivation.[2-4] We have identified a LQT2-associated missense mutation in a Spanish family, which results in the substitution of glutamic acid to the uncharged amino acid glycine at position 637 (p.E637G). Change of this residue to charged amino acids such as lysine (p.E637K) or aspartic acid (p.E637D) has been previously associated with LQT2,[5,6] although only the functional properties of p.E637K were studied.[5] p.E637K channels did not generate measurable currents in *Xenopus* oocytes, however when p.E637K and wild-type (WT) channels were coexpressed, currents generated displayed lower amplitude and small changes in the voltage dependence of activation, inactivation and K^+ selectivity compared to WT currents.

This study aims to determine the effects of the substitution of a negatively charged residue (E) located in the outer pore region by a neutral amino acid (G) on HERG channel properties and to identify the mechanism by which p.E637G mutation of Kv11.1 channels can lead to QT prolongation.

Methods

The study was approved by the Investigation Committee of the Hospital Universitario Virgen de las Nieves and conforms to the principles outlined in the Declaration of Helsinki. Informed consent was obtained for the genetic screening test. Genomic DNA was isolated from white blood cell by conventional methods. Polymerase chain reaction/single-strand conformation polymorphism analyses were used to screen for mutations in KCNQ1, KCNH2 and SCN5A. Human cardiac KCNH2 was kindly gifted by Dr. C. Bezzina (University of Amsterdam, The Netherlands).[7] p.E637G mutation was introduced using the QuikChange Site-Directed Mutagenesis kit (Stratagene, USA) as previously described.[8,9] WT and p.E637G channels were transiently transfected in CHO cells and currents were recorded using the whole-cell patch-clamp configuration.[8-10] For simulating the shapes of ventricular APs, we employed the Grandi-Bers model of a human ventricular AP.[11] Results are expressed as mean±SEM. Paired or unpaired *t* test or one-way ANOVA followed by Newman-Keuls test were used to assess statistical significance where appropriate. A value of $P<0.05$ was considered significant. A detailed Methods section is available online.

Results

Case description

A woman diagnosed with epilepsy since age 11, was referred to the Arrhythmias Unit for evaluation because of a ventricular fibrillation episode. She had been followed-up in the Epilepsy Unit with poor response to antiepileptic drugs. Indeed, she often suffered syncope in response to auditory stimuli such as the sound of the telephone. Magnetic resonance imaging of the head and electroencephalography showed no abnormal findings. At the age of 43, triggered by the buzzing of an alarm clock, she suddenly lost her conscious with no reaction to external stimuli. When the Emergencies Services arrived she was suffering a ventricular fibrillation which required external defibrillation with 200 J. The basal electrocardiogram of the proband showed a marked QT prolongation (Bazzett-corrected QT interval [QTc] of 560 ms) suggesting a LQT2 (Figure 1A). Her two daughters (aged 25 and 23) also presented prolonged QTc (Figures 1B, 1C) even when they are neurologically and cardiologically asymptomatic until yet.

Genetic analysis

Direct DNA sequence analysis from the proband identified a mutation at nucleotide 1910 of KCNH2 consisting of an adenine to guanine substitution. This mutation leads to an amino acid substitution from glutamic acid to glycine at position 637 of Kv11.1 channel (Figure 2B) and was not observed in the DNA samples of more than 200 control subjects. Sequence analysis of all the other exons of KCNH2 did not reveal any other mutation and screening for mutations in KCNQ1 and SCN5A was negative. Her two daughters presented the same mutation in KCNH2 (Figure 2A) and both of them were diagnosed of LQTS based on Schwartz score (>4 points).[1] The proband and her

daughters also carried a polymorphism (g.1956T>C) in KCNH2 which does not cause substitution in the encoded amino acid (Tyr652). Her sister, brother and parents, who did not have a prolonged QTc, did not present the mutation (Figure 2A). The penetrance of LQTS among the mutation carriers was 100 %.

Functional characterization of p.E637G channels

To determine the mechanism by which mutation p.E637G of Kv11.1 channels can lead to LQTS, we compared currents recorded in CHO cells expressing homotetrameric WT (I_{WT}) and p.E637G (I_{E637G}), or heterotetrameric WT/p.E637G ($I_{WT/E637G}$) channels. Currents were recorded using standardized protocols by applying 5 s-pulses from -80 mV to voltages between -80 and +60 mV in 10 mV increments. As shown in Figure 3A, WT Kv11.1 channels generated a slowly activating current (τ_{act}=951±85 ms at 0 mV, n=21) whose amplitude progressively increased with pulses up to 0 mV and then progressively decreased at potentials >0 mV due to the fast C-type inactivation,[12] resulting in the bell-shaped I-V curve typical of Kv11.1 channels (Figure 3B). p.E637G channels generated a current with significantly lower amplitude at potentials between -40 and +40 mV (Figures 3A and 3B). I_{E637G} amplitude at 0 mV was very small, which did not allow a reliable measurement of the activation kinetics. Therefore, it was measured at +40 mV yielding a τ_{act} value of 734±136 ms (n=8). Interestingly, I_{E637G} did not display inward rectification (Figures 3A and B), and thus, the I-V curve did not exhibit a bell-shaped morphology. When p.E637G and WT Kv11.1 channels were coexpressed, current generated did not exhibit inward rectification either, however it was larger than I_{E637G} at potentials ≥+20 ($P<0.05$, n=6) (Figure 3B).

Tail currents were recorded on repolarization to -60 mV for 5 s. A biexponential function was fitted to the tail current traces recorded after pulses to +60 mV yielding τ_f

and τ_s values of 221±27 and 1340±178 ms for WT Kv11.1 channels. p.E637G mutation did not modify tail current kinetics (Table 1). However, unlike WT, deactivating tail currents of p.E637G and WT/p.E637G Kv11.1 channels were inward over the range of voltages tested (Figure 3A), which suggested an alteration in K^+ selectivity. To examine if p.E637G mutation affected ion selectivity of the channel, we determined the reversal potential (E_{rev}) in cells expressing WT, p.E637G and WT/p.E637G Kv11.1 channels (Figure 4A, 4B, Table 1). The E_{rev} values were much more positive for p.E637G and WT/p.E637G than WT channels ($P<0.001$ vs WT), suggesting that p.E637G and WT/p.E637G channels were less selective for K^+ ions than WT channels.

Mean activation curves and the fit of a Boltzmann function to the data for WT, p.E637G and WT/p.E637G channels are depicted in Figure 4C. As mentioned above, the tail currents generated by p.E637G and WT/p.E637G channels were inward after pulses to potentials between -30 and +60 mV (Figure 4C). Normalized activation curves demonstrated that the mutation alone or when coexpressed with WT shifted the midpoint towards more positive potentials and decreased the slope of the curve ($P<0.05$) (Figure 4D, Table 1).

The loss of inward rectification strongly suggested that the p.E637G mutation disrupted the inactivation process of the channel. To confirm this hypothesis, we looked for changes in the steady-state inactivation (availability) of the channels using standardized protocols previously described (Online Figure I).[10] Figure 4E shows normalized corrected for closing inactivation curves for WT, p.E637G and WT/p.E637G channels together with the Boltzmann fits to the data. The V_h and k for WT channels were -62.3±5.9 mV and 28.1±1.3, respectively (Table 1). As expected, inactivation of both p.E637G and WT/p.E637G channels was greatly reduced compared to WT channels, in such a way that at +20 mV 93.1±0.7% of the WT channels were inactivated, while only

20.5±5.5 and 34.4±7.8% of p.E637G and WT/p.E637G channels, respectively, were inactivated at this potential (P<0.05 vs WT) (Figure 4E). Since dofetilide preferentially interacts with Kv11.1 channels in the inactivated state, we tested whether p.E637G mutation also affects Kv11.1 channel affinity for this drug. Blockade induced by 1 μM dofetilide in p.E637G, and WT/p.E637G was significantly smaller than in WT channels (Figure 4F).

Effects of the incubation of cells expressing p.E637G channels with pharmacological chaperones

Some reports have demonstrated that trafficking of Kv11.1 channel mutants can be restored by reducing the incubation temperature during cell culture[13] or by incubation with compounds (4-phenylbutyrate or glicerol) or drugs (dofetilide, terfenadine or its metabolite fexofenadine) that act as protein-stabilizing agents improving channel trafficking (pharmacological chaperones).[14] Reducing the incubation temperature during cell culture to 27ºC or incubation of the p.E637G transfected cells with 1 μM terfenadine or 1 μM dofetilide for 24 h did not modify current properties compared to that recorded under control conditions (not shown). Conversely, when p.E637G transfected cells were incubated with 1 μM fexofenadine (Figure 5A) or 5 mM 4-phenylbutyrate (Figure 5B), the current generated was larger but with the same time- and voltage-dependent features than those generated by non-incubated cells (n=8 in each group). Furthermore, the E_{rev} of I_{E637G} recorded in cells incubated with fexofenadine or 4-phenylbutyrate was similar to that obtained in non-incubated cells (Figure 5C, Table 1). I_{WT} recorded in cells incubated with fexofenadine or 4-phenylbutyrate were identical to those generated by non-incubated cells (Figure 5B).

Physiological consequences of p.E637G mutation

To determine the consequences of p.E637G mutation in a physiologically relevant setting, we used a human endocardial AP voltage clamp protocol (Figure 6A). In cells transfected with WT channels, current was small at the peak of the AP due to the rapid inactivation of the channels. However, as the voltage became less positive, amplitude of the outward current progressively increased reaching a maximum before the final declining phase of the AP. Cells transfected with either p.E637G or WT/p.E637G channels generated a small current that rapidly activated coinciding with the peak of the AP and progressively decreased as the voltage became more negative. Due to the loss of K^+ selectivity an inward depolarizing Na^+ current was produced during the final phase of repolarization. Therefore, the mutation significantly reduced the charge crossing the membrane estimated from the integral of the current traces compared to WT channels (Figure 6B). Furthermore, incubation of cells expressing p.E637G with fexofenadine or 4-phenylbutyrate, resulted in charge values larger than in non-incubated cells that were also significantly lower than those obtained in cells expressing WT channels (Figure 6B).

Simulation of the effects of p.E637G mutation on the cardiac AP

The effects of the mutation on the AP characteristics were simulated using a theoretical model of a human ventricular myocyte. The model was run for endocardial and epicardial cells at different frequencies ranging 0.1 and 3 Hz. Given the heterozygous nature of the disease, in the patient most of the channels will be heterotetramers of WT and p.E637G subunits. Therefore, the model was run considering the conductance of WT channels and also the conductance reduction (70.2%) produced by WT/p.E637G channels. Furthermore, the time constants, the midpoint and slope values of the

activation/inactivation curves and the E_{rev} for WT and WT/p.E637G channels were also incorporated.

As can be observed, currents obtained by incorporating these values were similar to those recorded experimentally (Figure 6C). As a consequence of the modifications in the current properties, the mutation prolonged the AP duration measured at 50 and 90% of repolarization (19.2 and 22.1%, respectively, at 1 Hz in endocardial cells) (Figure 6D). The AP duration prolongation was greater in endocardial than epicardial cells and at slow than at fast driving frequencies (inset of Figure 6D). Furthermore, neither early afterdepolarizations nor alternans of the APD were predicted by the model when it was run at 0.1 and 3 Hz, respectively. Conversely, alternans were observed when the epicardial and endocardial models were run in control conditions (Online Figure II).

Discussion

In this study, we have characterized a LQT2-associated missense mutation which implies a substitution of the glutamic acid to glycine at position 637, which is located in the outer mouth of the pore at the beginning of S6 (Figure 7B). The mutation abolished inward rectification by disrupting C-type inactivation of Kv11.1 channels and eliminated the K^+ selectivity. These alterations caused a marked decrease of the Kv11.1 current ($I_{Kv11.1}$) amplitude during the AP, which explains the QT prolongation observed in the carriers of this mutation.

p.E637 mutation alters channel gating

We have found a single base substitution (g.1910A>G) in the KCNH2 gene in a 43-year-old woman. The proband, who presented a marked prolongation of the QT interval, often suffered syncope in response to auditory stimuli and was diagnosed with LQT2 after a ventricular fibrillation episode. Genetic screening identified the same missense mutation in her two daughters that also presented QT prolongation, even when they are asymptomatic until yet. The proband had been diagnosed with epilepsy and treated unsuccessfully with oxcarbazepine for 32 years. Later, neurological data obtained after her reevaluation were not consistent with epilepsy. Furthermore, after the treatment with β-blockers was implemented, she did not experience any other cardiac or epileptic episode. Nevertheless, since Kv11.1 channels are also expressed in the central nervous system, we cannot discard the presence of neurally mediated seizures in patients carrying this mutation. Indeed growing evidence suggests a pathogenic link between LQTS and epilepsy, particularly in LQT2 patients.[2,15]

At physiologically relevant membrane potentials, the $I_{Kv11.1}$ amplitude recorded by applying depolarizing pulses in cells expressing p.E637G and WT/p.E637G channels was significantly smaller than that recorded in cells expressing WT channels. Importantly, coexpression of WT and mutant channels reduced current density by more than 50% compared with the expression of WT alone, suggesting that p.E637G mutation produced a dominant negative effect.

Moreover, the mutation induced severe alterations in the voltage dependence of activation (a positive shift in the midpoint and a marked change in the slope of the activation curve), a loss of channel selectivity (E_{rev} was shifted by ≈60 mV to more positive potentials), and a disruption of C-type inactivation (the current did not display inward rectification). Thus, our results support that the activation, inactivation and K^+ selectivity in Kv11.1 channels are functionally related,[16] and highlight the importance of the Glu637 residue in the control of these processes. Mutations in some amino acids of the outer mouth of the pore region of Kv11.1, comprising the extracellular portions of S5 and S6 domains and the pore loop, also modified channel voltage dependence of activation, disrupted C-type inactivation and eliminated K^+ selectivity.[16,17] Based on these results, it was proposed that this outer pore region, which is unique among voltage-dependent K^+ channels, is a key determinant of the special features of Kv11.1 channels.[16,18] In this regard, it seems that the conformational flexibility of this region, as a consequence of a reduced hydrogen bonding capability, is an important contributing factor.[186] Therefore, it could be possible that the introduction of a glycine at position 637 increases the hydrogen bonding capability which, in turn, is detrimental to C-type inactivation. Indeed, Glu637, which is highly conserved among the Kv11.x channel family, is substituted by a glycine in other voltage-gated K^+ channels such as Kv1.5 or

Kv7.1 (Figure 7A), which displays inactivation properties very different from those of Kv11.1.

Hayashi *et al* described the effects produced by another mutation at this position (p.E637K) and found somewhat different results.[5] They showed that expression of p.E637K in *Xenopus* oocytes did not produce detectable currents. However, coexpression of p.E637K and WT Kv11.1 channels generated inward rectifying currents with small modifications in their biophysical properties. Indeed, they described a positive shift in the voltage dependence of activation without variations in the slope of the activation curve, a negative shift in the voltage dependence of inactivation and a 6 mV-positive shift in the E_{rev} compared to WT channels. The apparent discrepancies between our results and those obtained by Hayashi *et al* could be attributed to the different amino acid for which the glutamic acid is substituted (Lys *vs* Gly).

It has been described that defective Kv11.1 channel trafficking can cause LQT2 in most cases.[219] Furthermore, some reports demonstrated that trafficking of these mutants can be restored by reducing the incubation temperature during cell culture[13] or by incubation with unspecific chaperones (4-phenylbutyrate) and high- (terfenadine, dofetilide) or low-affinity (fexofenadine) Kv11.1 channel blockers.[14,19] Expression of p.E637G channels was not modified either by reducing the incubation temperature during cell culture or by incubation with terfenadine or dofetilide. The latter could be attributed to the low affinity for p.E637G channels exhibited by dofetilide, which in turn is probably due to the fact that dofetilide is an inactivated-state Kv11.1 blocker and p.E637G channels do not inactivate. Conversely, incubation with fexofenadine and 4-phenylbutyrate significantly increased current amplitude and density, without affecting

the biophysical features of p.E637G channels, i.e. absence of inward rectification, disruption of inactivation, and loss of K^+ selectivity.

Physiological consequences of the mutation

The alterations in the channel gating induced by the p.E637G mutation produced a marked reduction in $I_{Kv11.1}$ amplitude during an AP leading to a delayed repolarization. Indeed, the charge crossing the membrane was reduced in mutant channels. Interestingly, when integrating all the alterations induced by the mutation in a simulated human ventricular AP, a marked lengthening of the AP duration was produced, which correlates with the QT prolongation observed in the mutation carriers. It may seem surprising that a mutation that reduces inactivation can prolong AP duration. However, it should be considered that loss of Kv11.1 channel inactivation leads to the elimination of the outward tail current produced by the fast recovery of inactivated channels upon repolarization.[17] Moreover, it is possible that the positive shift of E_{rev} induced by p.E637G mutation can also contribute to the delay in the repolarization process.[17] Indeed, Na^+ ions can be carried through these mutant channels, resulting in an inward current at the end of repolarization, as shown by the AP-clamp experiments. The AP prolongation may result in the development of early afterdepolarizations, which can lead to severe ventricular arrhytmias. However, in the model used, neither early afterdepolarizations nor alternans were generated in epicardial and endocardial cells. Importantly, the prolongation induced by the mutation was greater in endocardial than epicardial cells, especially at slow frequencies. This fact suggests that the mutation would exacerbate the transmural dispersion of repolarization, which has been identified as the principal arrhythmogenic substrate in LQTS.[20]

Recent data have demonstrated the relevance of the location, coding type and topology of the mutation in order to predict the clinical phenotype of the patient.[21,22] Indeed, the QTc is longer and cardiac events are more frequent in patients with mutations in the transmembrane pore region (comprising S5 and S6 segments and the P-loop) than in patients with mutations in transmembrane nonpore (S1 to S4), N- or C-terminus regions, in patients with missense mutations than in patients with either frameshift/nonsense or other mutations, and in patients with mutations located in α-helical domains than among patients with mutations in β-sheet domains or other uncategorized locations.[21] Therefore, p.E637G is a high risk mutation considering that is missense and is located in the α-helical domain of the S6 segment.

Conclusion

We have identified a LQT2-associated mutation that through removal of C-type inactivation and reduction of K^+ selectivity decreases outward repolarizing current during the AP, leading to a marked delay of repolarization. Moreover, the results obtained demonstrate the importance of Glu637 in the inactivation process and ion selectivity of Kv11.1 channels.

References

1. Roden DM. Clinical practice. Long-QT syndrome. N Engl J Med 2008;358:169-176.
2. Sanguinetti MC. HERG1 channelopathies. Pflugers Arch 2010;460:265-276.
3. Zhao JT, Hill AP, Varghese A, et al. Not all hERG pore domain mutations have a severe phenotype: G584S has an inactivation gating defect with mild phenotype compared to G572S, which has a dominant negative trafficking defect and a severe phenotype. J Cardiovasc Electrophysiol 2009;20:923-930.
4. Shushi L, Kerem B, Goldmit M, et al. Clinical, genetic, and electrophysiologic characteristics of a new PAS-domain HERG mutation (M124R) causing Long QT syndrome. Ann Noninvasive Electrocardiol 2005;10:334-341.
5. Hayashi K, Shimizu M, Ino H, et al. Characterization of a novel missense mutation E637K in the pore-S6 loop of HERG in a patient with long QT syndrome. Cardiovasc Res 2002;54:67-76.
6. Napolitano C, Priori SG, Schwartz PJ, et al. Genetic testing in the long QT syndrome: development and validation of an efficient approach to genotyping in clinical practice. JAMA 2005;294:2975-2980.
7. Bezzina CR, Verkerk AO, Busjahn A, et al. A common polymorphism in KCNH2 (HERG) hastens cardiac repolarization. Cardiovasc Res 2003;59:27-36.
8. Gómez R, Caballero R, Barana A, et al. Nitric oxide increases cardiac I_{K1} by nitrosylation of cysteine 76 of Kir2.1 channels. Circ Res 2009;105:383-392.
9. Caballero R, Dolz-Gaitón P, Gómez R, et al. Flecainide increases Kir2.1 currents by interacting with cysteine 311 decreasing the polyamine-induced rectification. Proc Natl Acad Sci USA 2010;107:15631-15636.

10. Caballero R, Moreno I, González T, et al. Spironolactone and its main metabolite, canrenoic acid, block human ether-a-go-go-related gene channels. Circulation 2003;107:889-895.
11. Grandi E, Pasqualini FS, Bers DM. A novel computational model of the human ventricular action potential and Ca^{2+} transient. J Mol Cell Cardiol 2010;48:112-121.
12. Spector PS, Curran ME, Zou A, Keating MT, Sanguinetti MC. Fast inactivation causes rectification of the I_{Kr} channel. J Gen Physiol 1996;107:611-619.
13. Paulussen A, Raes A, Matthijs G, Snyders DJ, Cohen N, Aerssens J. A novel mutation (T65P) in the PAS domain of the human potassium channel HERG results in the long QT syndrome by trafficking deficiency. J Biol Chem 2002;277:48610-48616.
14. Rajamani S, Anderson CL, Anson BD, January CT. Pharmacological rescue of human K^+ channel long-QT2 mutations: human ether-a-go-go-related gene rescue without block. Circulation 2002;105:2830-2835.
15. Johnson JN, Hofman N, Haglund CM, Cascino GD, Wilde AA, Ackerman MJ. Identification of a possible pathogenic link between congenital long QT syndrome and epilepsy. Neurology 2009;72:224-231.
16. Liu J, Zhang M, Jiang M, Tseng GN. Structural and functional role of the extracellular S5-P linker in the HERG potassium channel. J Gen Physiol 2002;120:723-737.
17. Lees-Miller JP, Duan Y, Teng GQ, Thorstad K, Duff HJ. Novel gain-of-function mechanism in K^+ channel-related long-QT syndrome: altered gating and selectivity in the HERG1 N629D mutant. Circ Res 2000;86:507-513.

18. Ju P, Pages G, Riek RP, et al. The pore domain outer helix contributes to both activation and inactivation of the HERG K^+ channel. J Biol Chem 2009;284:1000-1008.

19. Anderson CL, Delisle BP, Anson BD, et al. Most LQT2 mutations reduce Kv11.1 (hERG) current by a class 2 (trafficking-deficient) mechanism. Circulation 2006;113:365-373.

20. Antzelevitch C. Ionic, molecular, and cellular bases of QT-interval prolongation and torsade de pointes. Europace 2007;9 Suppl 4:iv4-iv15.

21. Shimizu W, Moss AJ, Wilde AA, et al. Genotype-phenotype aspects of type 2 long QT syndrome. J Am Coll Cardiol 2009;54:2052-2062.

22. Kapa S, Tester DJ, Salisbury BA, et al. Genetic testing for long-QT syndrome: distinguishing pathogenic mutations from benign variants. Circulation 2009;120:1752-1760.

Table 1. Time- and voltage-dependent properties of WT and mutant Kv11.1 channels.

	Activation			Deactivation		Inactivation		E_{rev} (mV)
	V_h (mV)	*k* (mV)	τ_{act} (ms)	τ_f (ms)	τ_s (ms)	V_h (mV)	*k* (mV)	
WT	-11.9±2.1	10.2±1.2	951±85	221±27	1340±178	-62.3±5.9	28.1±1.3	-78.3±0.7
p.E637G	-1.9±2.9*	22.7±4.6*	734±136	160±35	1271±300	-5.9±2.4*	4.8±1.3*	-17.8±0.9*
WT/p.E637G	-3.1±2.0*	18.6±2.9*	1025±200	238±55	1996±453	-30.8±5.3*†	10.0±5.1*	-18.4±4.0*
p.E637G (Fexof)	-0.9±1.6*	19.7±3.2*	998±120	176±26	1262±167	-7.1±5.1*	3.8±5.4*	-20.5±1.4*
p.E637G (4-PB)	-2.3±2.9*	19.7±4.2*	899±163	166±26	1264±268	-5.8±4.9*	4.7±3.9*	-18.3±3.2*

V_h and *k*: midpoint and slope values of the activation/inactivation curves.
τ_{act}: time constant of activation, measured at 0 mV in WT and at +40 mV in the rest of the constructs.
τ_f and τ_s: fast and slow time constants of deactivation of tail currents at -60 mV recorded after pulses to +60 mV.
* P<0.05 vs WT. † P<0.05 vs p.E637G

Figure legends

Figure 1. Twelve-lead electrocardiogram of the proband **(A)** and her two daughters **(B and C)** showing a marked QT prolongation (A: 560 ms; B: 490 ms; C: 550 ms).

Figure 2. A, Pedigree of the proband´s family. The arrow indicates the proband, black symbols indicate presence of the mutation (heterozygosis). Males are shown as squares and females as circles. **B,** DNA sequence analysis in the proband. The same single nucleotide substitution from adenine to guanine (arrow) was observed in the three affected patients.

Figure 3. Traces obtained by applying the protocol shown at the top **(A)** and current density-voltage relationships **(B)** for currents recorded in cells transfected with WT, p.E637G, and WT/p.E637G Kv11.1 channels. Each point represents the mean±SEM of ≥ 6 experiments. * P<0.05 vs WT; ϕ P<0.05 vs p.E637G.

Figure 4. A, I_{WT} traces recorded by applying 500 ms-pulses from -80 to +20 mV followed by repolarization to voltages between -95 and -75 mV in 5 mV increments. **B,** Normalized amplitude of tail currents recorded in cells expressing WT, p.E637G, and WT/p.E637G on return to potentials between -95 and -75 mV or between –35 and -15 mV, respectively. Mean **(C)** and normalized **(D)** activation curves as calculated from peak tail-current amplitudes recorded on return to -60 mV in cells expressing WT, p.E637G, and WT/p.E637G. **E,** Corrected for closing inactivation curves constructed by plotting the initial current at +40 mV recorded in cells expressing WT, p.E637G, and WT/p.E637G Kv11.1 channels. In C and E, * P<0.05 vs WT. **F,** Dofetilide (1 μM)-

induced block measured as reduction of the amplitude of the tail currents recorded at -60 mV after pulses to +60 mV in WT, pE637G, and WT/p.E637G channels. *** P<0.001 vs WT. Each point/bar represents mean±SEM of ≥6 experiments.

Figure 5. A, Current traces recorded by applying the protocol shown at the top in cells transfected with p.E637G Kv11.1 channels incubated with 1 μM fexofenadine for 24 h. **B,** Current density-voltage relationships for currents recorded in cells transfected with p.E637G Kv11.1 channels incubated or not with 1 μM fexofenadine (Fexof) and 5 mM 4-phenylbutyrate (4-PB). *P<0.05 vs non-incubated cells. Dotted and dashed lines represent current density-voltage relationships for WT Kv11.1 channels incubated with fexofenadine and 4-phenylbutyrate, respectively. **C,** Mean E_{rev} for currents recorded in cells expressing WT or p.E637G incubated with fexofenadine and 4-phenylbutyrate. *** P<0.001 vs WT. Each point/bar represents mean±SEM of ≥6 experiments.

Figure 6. A, Current traces elicited by AP command signals (top) as voltage protocol recorded in cells expressing WT or WT/p.E637G channels. **B,** Mean charge crossing the membrane through WT or mutant Kv11.1 channels. Each bar represents the mean±SEM of ≥6 experiments. ** P<0.01 vs WT; ϕ P<0.05 vs p.E637G. Current traces **(C)** and AP **(D)** simulated using the Grandi-Bers model of ventricular AP by incorporating data from WT or WT/p.E637G Kv11.1 channels. The inset in D shows the frequency dependence of the AP duration prolongation.

Figure 7. A, Amino acid sequence alignments of the S6 domain of several voltage-dependent K^+ channels. **B,** Molecular modeling of S5 and S6 segments of Kv11.1

channels using the crystalized structure of Kv1.2 as a template showing the location of Glu637 residue (red).

Figure 1

Click here to download high resolution image

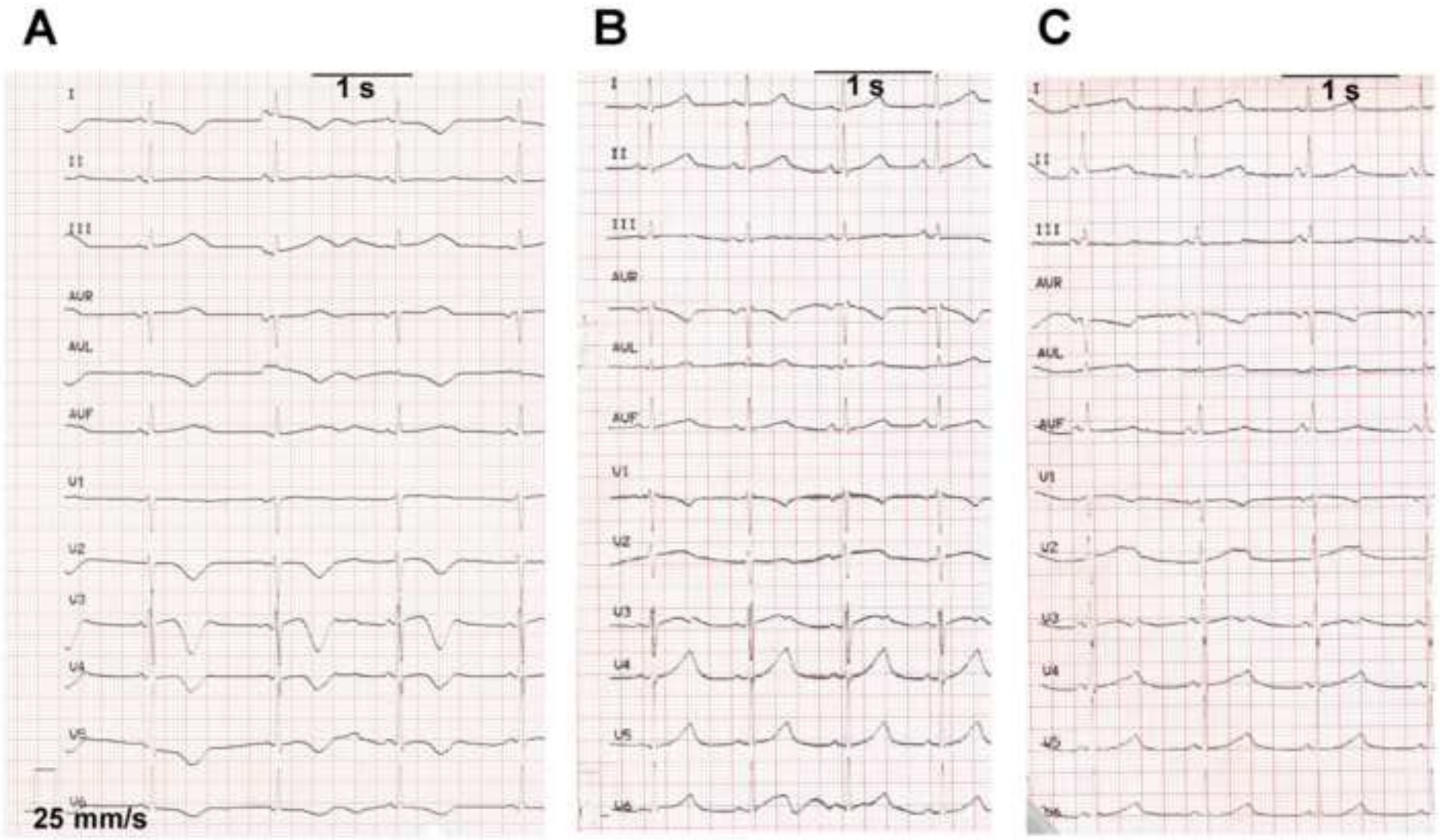

Figure 1

Figure 2

Click here to download high resolution image

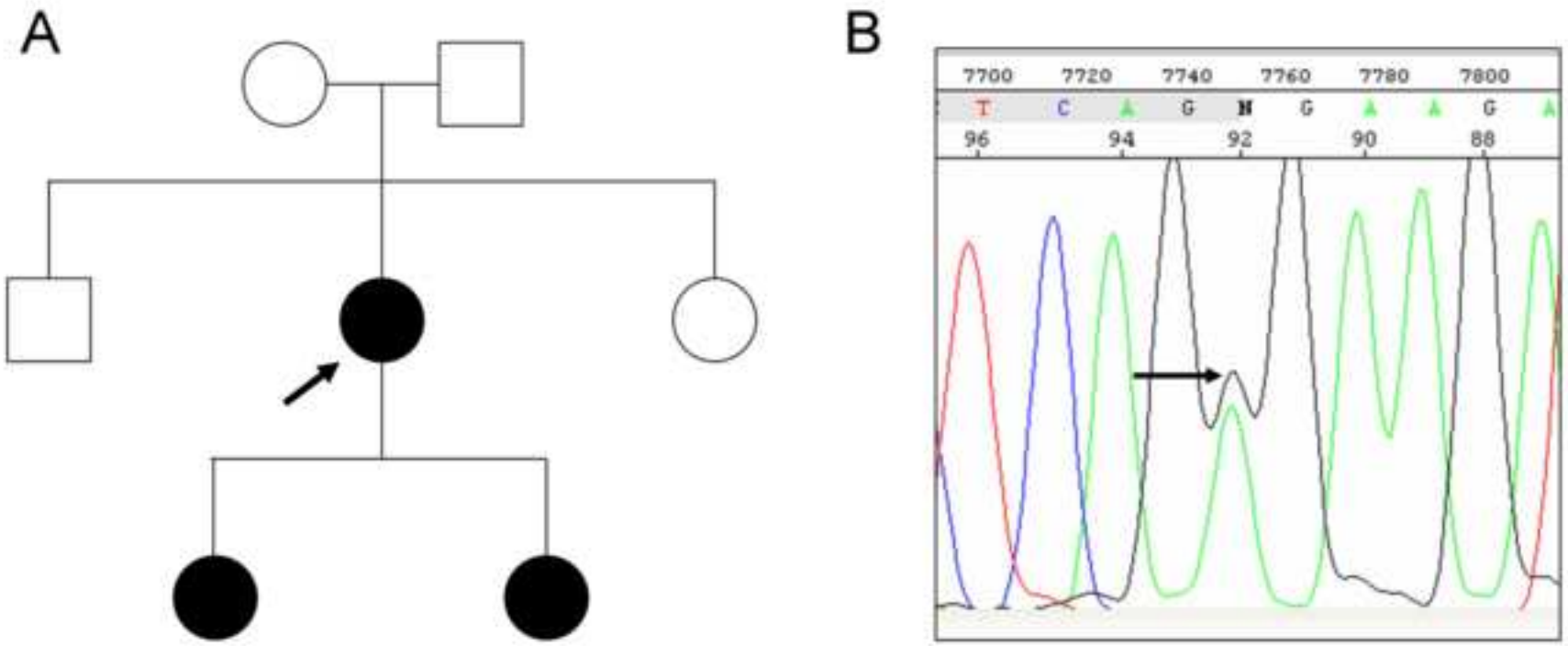

Figure 2

Figure 3

Click here to download high resolution image

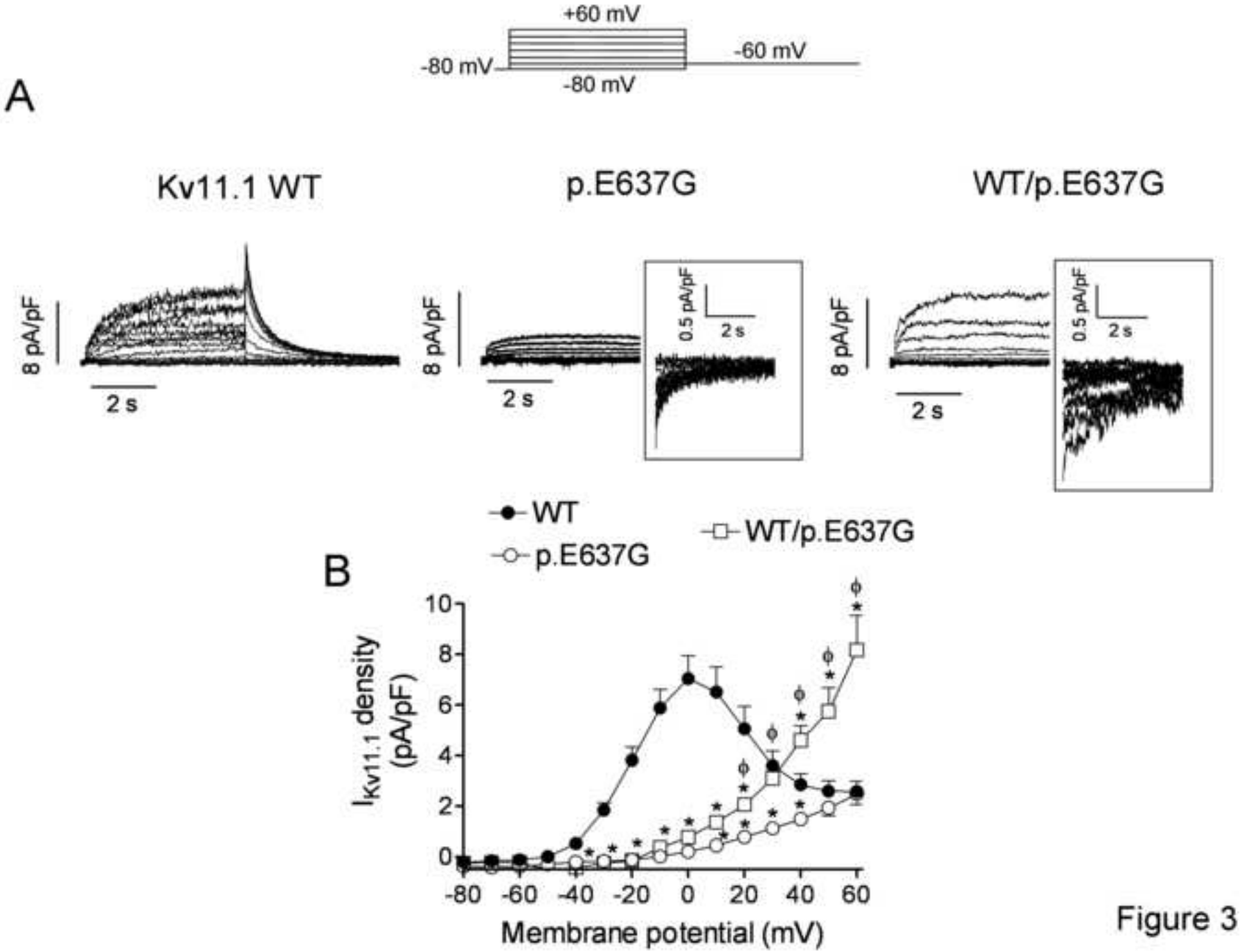

Figure 3

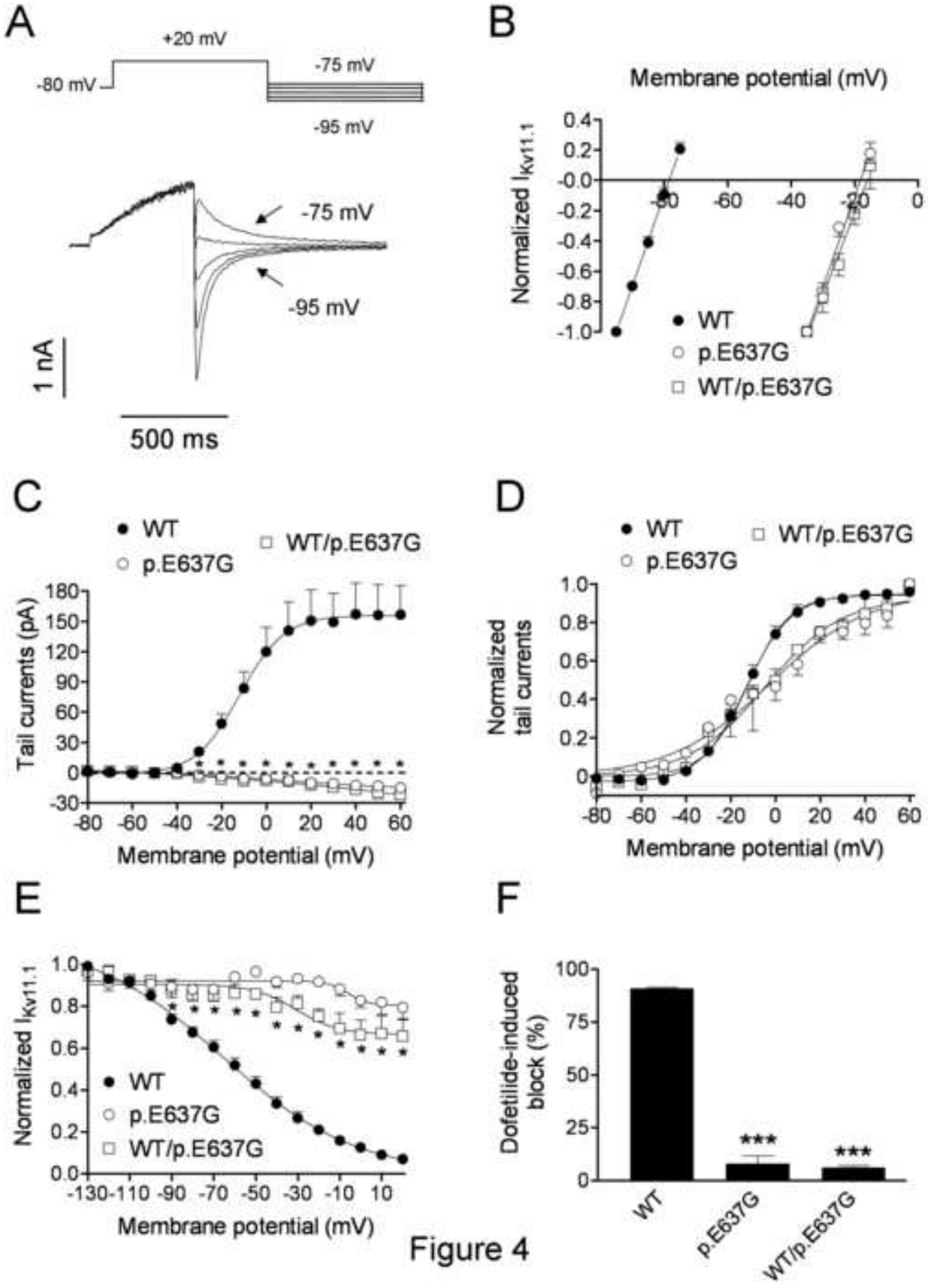
A
+20 mV
-75 mV
-80 mV
-95 mV
-75 mV
-95 mV
1 nA
500 ms
B
Membrane potential (mV)
Normalized $I_{Kv11.1}$
WT
p.E637G
WT/p.E637G
C
WT
p.E637G
WT/p.E637G
Tail currents (pA)
Membrane potential (mV)
D
WT
p.E637G
WT/p.E637G
Normalized tail currents
Membrane potential (mV)
E
Normalized $I_{Kv11.1}$
WT
p.E637G
WT/p.E637G
Membrane potential (mV)
F
Dofetilide-induced block (%)
***
***
WT
p.E637G
WT/p.E637G

Figure 4

Figure 5

Click here to download high resolution image

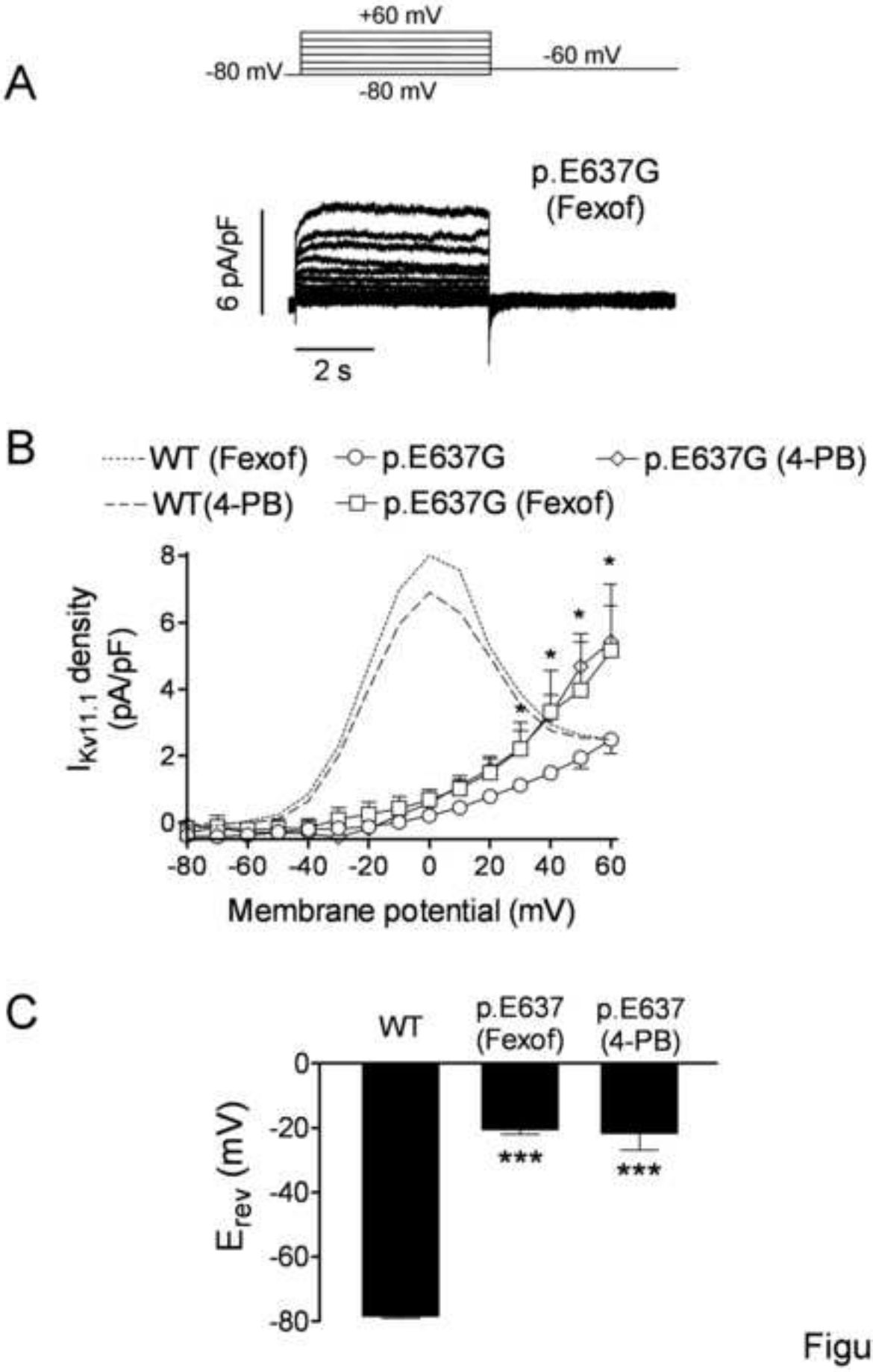

Figure 5

Figure 6

Click here to download high resolution image

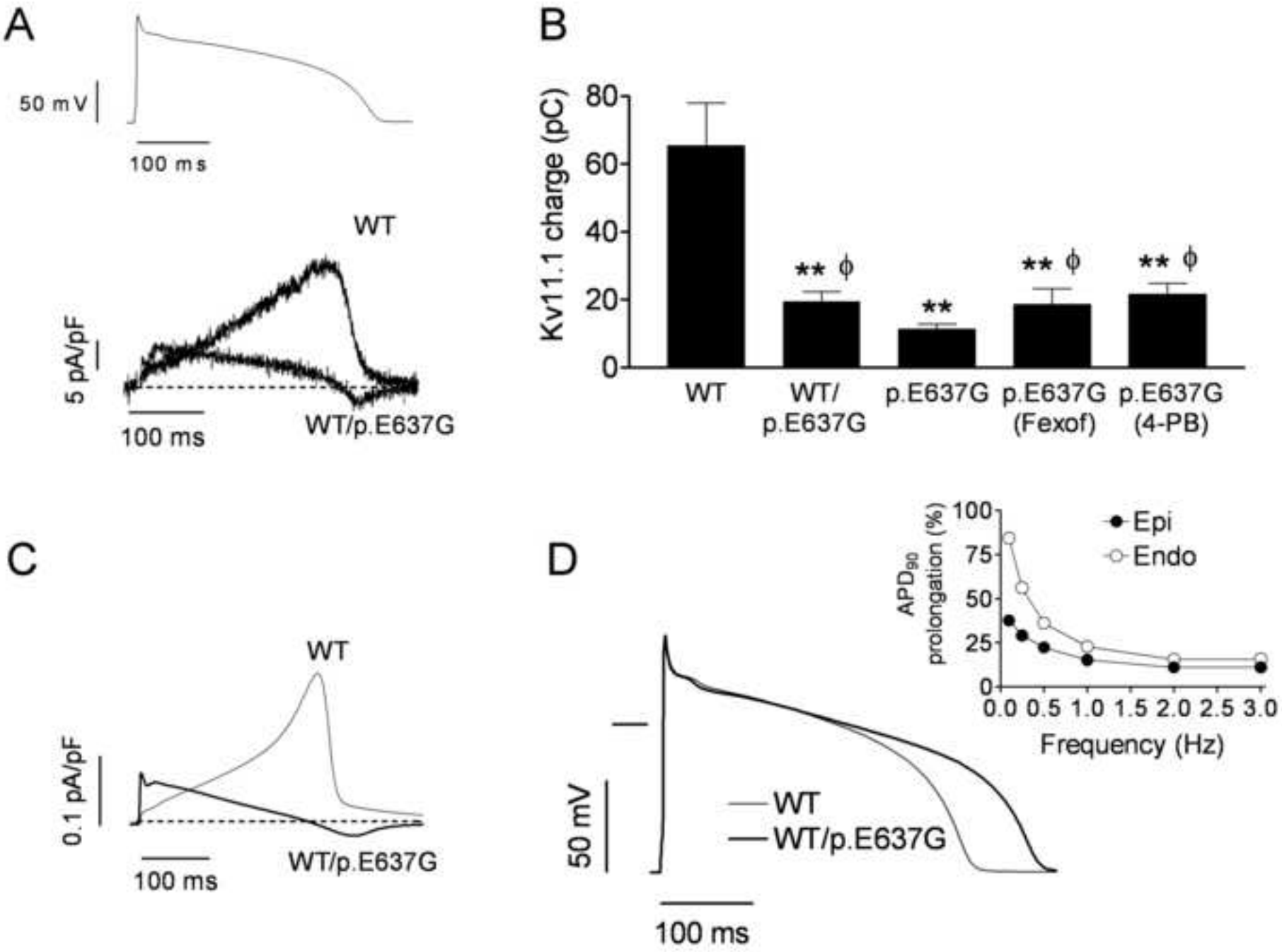

Figure 6

Figure 7

Click here to download high resolution image

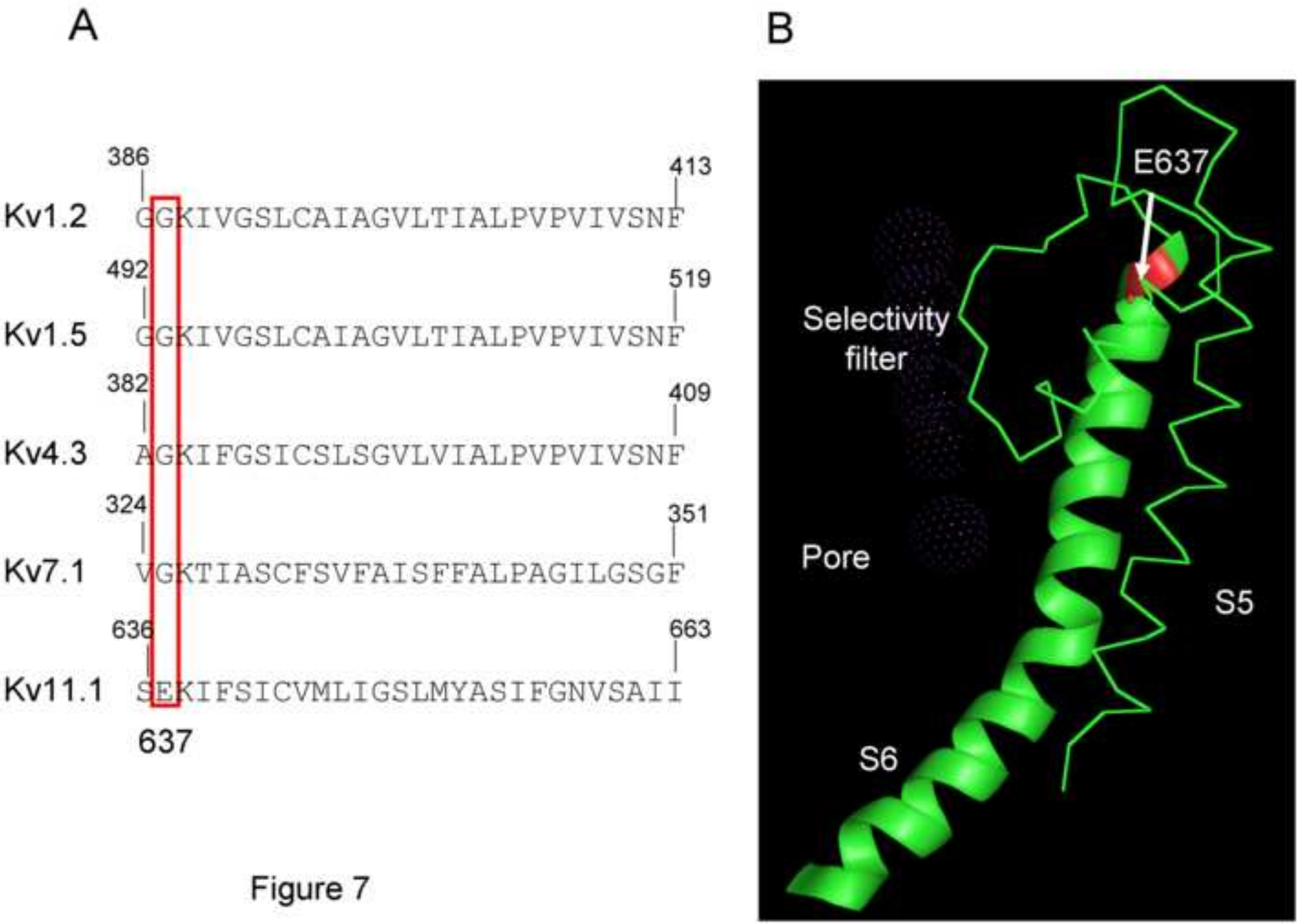

Figure 7

Supplementary material

Expanded methods

DNA isolation and mutation analysis

Informed consent was obtained for the genetic screening test. Genomic DNA was isolated from white blood cell nuclei by conventional methods. Polymerase chain reaction/single-strand conformation polymorphism (PCR-SSCP) analyses were used to screen for mutations in KCNQ1, KCNH2 and SCN5A genes. All the exons were sequenced using previously published primers.[1] PCR products were purified and applied to an agarose gel. Amplified DNA sequencing was conducted using ABI PRISM BigDye v3.1 (PE Applied Biosystems, Foster City, CA, USA).

Site-Directed Mutagenesis

Human cardiac Kv11.1 cDNA was kindly gifted by Dr. C. Bezzina (University of Amsterdam, The Netherlands).[2] p.E637G mutation was introduced using the QuikChange Site-Directed Mutagenesis kit (Stratagene, USA) as previously described.[3,4] The mutation was confirmed by direct DNA sequencing.

Cell culture and transfections

CHO cells were cultured and transfected as previously described.[3-5] Cells were grown in Ham-F12 medium supplemented with 10% fetal bovine serum, 100 U/mL penicillin, and 100 µg/mL streptomycin. The cultures were passaged every 4–5 days using a brief trypsin treatment. CHO cells were transiently transfected with the cDNA encoding WT or p.E637G Kv11.1 channels (1 µg) together with the cDNA encoding the CD8 antigen (0.5 µg) by using FUGENE6 (Roche Diagnostics, Switzerland) following manufacturer

instructions. In some experiments WT and p.E637G were coexpressed at 1:1 ratio (WT/p.E637G). For culture and transfections, 60 mm culture dishes were used. After 48 h, cells were incubated with polystyrene microbeads precoated with anti-CD8 antibody (Dynabeads M450; Dynal, Norway). Most of the cells that were beaded also had channel expression. The cells were removed from the dish with a cell scraper and the cell suspension was stored at room temperature and used within 12 h for electrophysiological experiments.

Recording techniques[3-9]

A small aliquot of cell suspension was placed in a 0.5 mL chamber mounted on the stage of an inverted microscope (Nikon TMS, Nikon Co., Japan). After settling to the bottom of the chamber, cells were perfused at 1 mL/min with external solution (see composition below). Macroscopic currents were recorded at room temperature (21-23ºC) using the whole cell patch-clamp technique with an Axopatch-200B patch-clamp amplifier (Molecular Devices, USA) (1-8). Recording pipettes were pulled from 1.0 mm o.d. borosilicate capillary tubes (GD1, Narishige Co., Ltd, Japan) using a programmable patch micropipette puller (Model P-2000 Brown-Flaming, Sutter Instruments Co., USA) and were heat-polished with a microforge (Model MF-83, Narishige). Micropipette resistance was <3.5 MΩ when filled with the internal solution and immersed in the external solution. The capacitive transients elicited by symmetrical 10 mV steps from 0 mV were recorded at 50 kHz (filtered at 10 kHz) for subsequent calculation of capacitative surface area, access resistance and input impedance. In all the experiments, series resistance was compensated manually by using the series resistance compensation unit of the Axopatch amplifier, and ≥80% compensation was achieved. In CHO cells, uncompensated access resistance and cell capacitance were 1.6±0.4 MΩ, and 16.7±1.8

pF, respectively (n=21), whereas maximum tail current amplitudes recorded at -60 mV after pulses to +60 mV in cells expressing WT channels averaged 198.9±37.8 pA (n=21). Thus, under our experimental conditions no significant voltage errors (<5 mV) due to series resistance were expected with the micropipettes used. The current recordings were sampled at 0.2 kHz and stored on the hard disk of a computer for subsequent analysis. Recording pipettes were filled with an internal solution containing (mM): K-aspartate 80, KCl 42, KH_2PO_4 10, MgATP 5, phosphocreatine 3, HEPES 5, and EGTA 5 (pH 7.2 with KOH). To record Kv11.1 currents ($I_{Kv11.1}$), CHO cells were perfused with an external solution containing (mM): NaCl 136, KCl 4, $CaCl_2$ 1.8, $MgCl_2$ 1, HEPES 10, and glucose 10 (pH 7.4 with NaOH). Under these conditions current amplitudes were stable during the time of recordings.[8,9]

Pulse protocols and analysis

The protocol to obtain current-voltage (I-V) curves consisted of 5-s pulses in 10 mV increments from a holding potential of –80 mV to potentials between −80 and +60 mV. Between −80 and −40 mV, only passive linear leak was observed, and least-squares fits to these data were used for passive leak correction. I-V curves were constructed by plotting the current amplitude measured at the end of the depolarizing pulses as a function of membrane potential. Deactivating tail currents were recorded at −60 mV and the activation curves were constructed by plotting peak tail current amplitudes as a function of the voltage of the preceding pulse. In some experiments, the effects of dofetilide (1 μM) were studied in WT, pE637G, and WT/p.E637G channels. Blockade induced by dofetilide was measured as reduction of the amplitude of the tail currents recorded at -60 mV after pulses to +60 mV.

The protocol to obtain the inactivation curves consisted of a first 1 s-pulse to +40 mV in order to activate the channels. Afterwards, the membrane voltage was stepped briefly (20 ms) to various test voltages (-130 and +20 mV) and then to +40 mV (480 ms). During the brief step, the inactivation process relaxed rapidly to the steady-state level appropriate to the test potential. The initial current on stepping to +40 mV gave the relative number of open channels. Thus, inactivation curves were constructed by plotting the current amplitude at +40 mV as a function of the interpulse potential. At negative potentials, the currents decline because significant closing of channels occurred through deactivation. For this reason, current amplitude at these voltages was corrected for by extrapolating the exponential falling phase back to the start of the negative voltage step and applying the same relative correction to the initial outward current. This procedure was used previously for the same purpose.[8] The activation and inactivation curves were fitted with a Boltzmann distribution:

$$y = A/\{1 + \exp[(V_h - V_m)/k]\}$$

where A is the amplitude term, V_h is the midpoint of activation or inactivation, V_m is the test potential, and k represents the slope factor of the curve.

To measure the reversal potential, a depolarizing pulse from a holding potential of −80 mV to +20 mV for 500 ms followed by repolarizing pulses from -95 to -75 mV (WT) or -35 to -15 mV (p.E637G and WT/p.E637G) in 5-mV increments was applied. The reversal potential was measured as the zero intercept of X-axis of the linear fit to the instantaneous tail currents at voltages bracketing the reversal potential.

I_{WT}, I_{E637G}, and $I_{WT/E637G}$ were also recorded by applying a human ventricular endocardial action potential (AP) waveform generated by using the Grandi-Bers model.

The amplitude and duration of the AP measured at 90% of repolarization were 128 mV and 334 ms, respectively (Grandi-Bers; Hancox). Therefore, the total charge crossing the membrane estimated from the integral of the current traces elicited by the AP was measured in each case.

Mathematical modeling of a ventricular AP

For simulating the shapes of ventricular AP, we employed the Grandi-Bers model of a human ventricular AP.[10] Simulated APs were implemented with MATLAB6.5 (Mathworks Inc., Natick, MA, USA) using the ode15s integration algorithm. Epicardial and endocardial model cells were paced at different frequencies ranging 0.1 and 2 Hz and currents and ionic concentrations were allowed to stabilized for at least 200 cycles. Under these conditions, the model was stable and reproduced the results obtained by Grandi et al in the description of the model.[10]

For WT/p.E637G, the model was run by incorporating the specific conductance (70.2% of reduction), the time constants and the midpoint and slope values of the activation/inactivation curves and the E_{rev} obtained in each case.

Drugs

Terfenadine, fexofenadine and 4-phenylbutyrate (Sigma) were initially dissolved in dimethylsulfoxide to yield 10 mM stock solutions. Dofetilide was kindly provided by Pfizer (United Kingdom) and dissolved following manufacturer instructions. In some experiments, CHO cells expressing WT, p.E637G and WT/p.E637G Kv11.1 channels were cultured (as described above) in the presence of 1 μM dofetilide, 1 μM fexofenadine, 1 μM terfenadine or 5 mM 4-phenylbutyrate for 24 h. The final concentration of the drugs was made by adding the stock solution to the culture

medium. Simultaneously, another batch of transfected cells was cultured in the presence of the same solvent concentration as in the drug-incubated cells. Drug or solvent were removed by culturing cells for 1 h in drug/solvent-free medium at 37ºC before electrophysiological recordings. In a different set of experiments, incubation temperature of the cells expressing WT, p.E637G and WT/p.E637G Kv11.1 channels was reduced to 27ºC.

Statistical methods

Results are expressed as mean±SEM. Paired or unpaired *t* test or one-way ANOVA followed by Newman-Keuls test were used to assess statistical significance where appropriate. A value of $P<0.05$ was considered significant.

Supplemental Results

Effects of p.E637G mutation on a simulated human ventricular AP.

Online Figure II shows superimposed traces of two consecutive epicardial APs obtained by running the Grandi-Bers model at 3 Hz under basal conditions (A) or after integrating all the I_{Kr} modifications induced by the p.E637G mutation (B). Under control conditions, AP duration (APD) alternans (ΔAPD_{90} for two consecutive beats= 8 ms) was observed, which correlates with $[Ca^{2+}]_i$ transients and I_{to} amplitude alternans (C and E). Interestingly, alternans was not apparent when the alterations induced by the mutation were considered (B, D, and F). Identical results were obtained when the endocardial model under control conditions and in the presence of the mutation were run (not shown). Alternans has been related not only with intracellular Ca^{2+} handling alterations but also with APD restitution slope (which reflects ion channel kinetics).[11] Thus, it is possible that the decreased I_{Kr} conductance induced by the mutation may lead to a dynamic change in the $[Ca^{2+}]_i$ secondary to the change in the morphology of the AP. Indeed, it has been demonstrated that a change in the contribution of any membrane current modifies the stability of the Ca^{2+} handling system and, in turn, should change the conditions under which Ca^{2+} alternans and, therefore, electrical alternans occur.[11,12] Therefore, it could be possible that the lengthening of the APD produced by the reduction of the I_{Kr} conductance influences the stability of the Ca^{2+} handling system reducing the Ca^{2+} alternans and the electrical alternans.

References

1. Splawski I, Shen J, Timothy KW, Vincent GM, Lehmann MH, Keating MT. Genomic structure of three long QT syndrome genes: *KVLQT*1, *HERG*, and *KCNE*1. Genomics 1998;51:86–97.
2. Bezzina CR, Verkerk AO, Busjahn A, et al. A common polymorphism in KCNH2 (HERG) hastens cardiac repolarization. Cardiovasc Res 2003;59:27-36.
3. Gómez R, Caballero R, Barana A, et al. Nitric oxide increases cardiac I_{K1} by nitrosylation of cysteine 76 of Kir2.1 channels. Circ Res 2009;105:383-392.
4. Caballero R, Dolz-Gaitón P, Gómez R, et al. Flecainide increases Kir2.1 currents by interacting with cysteine 311 decreasing the polyamine-induced rectification. Proc Natl Acad Sci USA. 2010;107:15631-15636.
5. Amorós I, Barana A, Caballero R, et al. Endocannabinoids and cannabinoid analogues block human cardiac Kv4.3 channels in a receptor-independent manner. J Mol Cell Cardiol 2010;48:201-210.
6. Caballero R, de la Fuente MG, Gómez R, et al. In humans, chronic atrial fibrillation decreases the transient outward current and ultrarapid component of the delayed rectifier current differentially on each atria and increases the slow component of the delayed rectifier current in both. J Am Coll Cardiol 2010;55:2346-2354.
7. Barana A, Amorós I, Caballero R, et al. Endocannabinoids and cannabinoid analogues block cardiac hKv1.5 channels in a cannabinoid receptor-independent manner. Cardiovasc Res 2010;85:56-67.
8. Caballero R, Moreno I, González T, et al. Spironolactone and its main metabolite, canrenoic acid, block human ether-a-go-go-related gene channels. Circulation 2003;107:889-895.

9. Moreno I, Caballero R, González T, et al. Effects of irbesartan on cloned potassium channels involved in human cardiac repolarization. J Pharmacol Exp Ther 2003;304:862-873.
10. Grandi E, Pasqualini FS, Bers DM. A novel computational model of the human ventricular action potential and Ca^{2+} transient. J Mol Cell Cardiol. 2010;48:112-121.
11. Jordan PN, Christini DJ. Action potential morphology influences intracellular calcium handling stability and the occurrence of alternans. Biophys J. 2006;90:672-680.
12. Jordan PN, Christini DJ. Characterizing the contribution of voltage- and calcium-dependent coupling to action potential stability: implications for repolarization alternans. Am J Physiol Heart Circ Physiol. 2007;293:H2109-H2118.

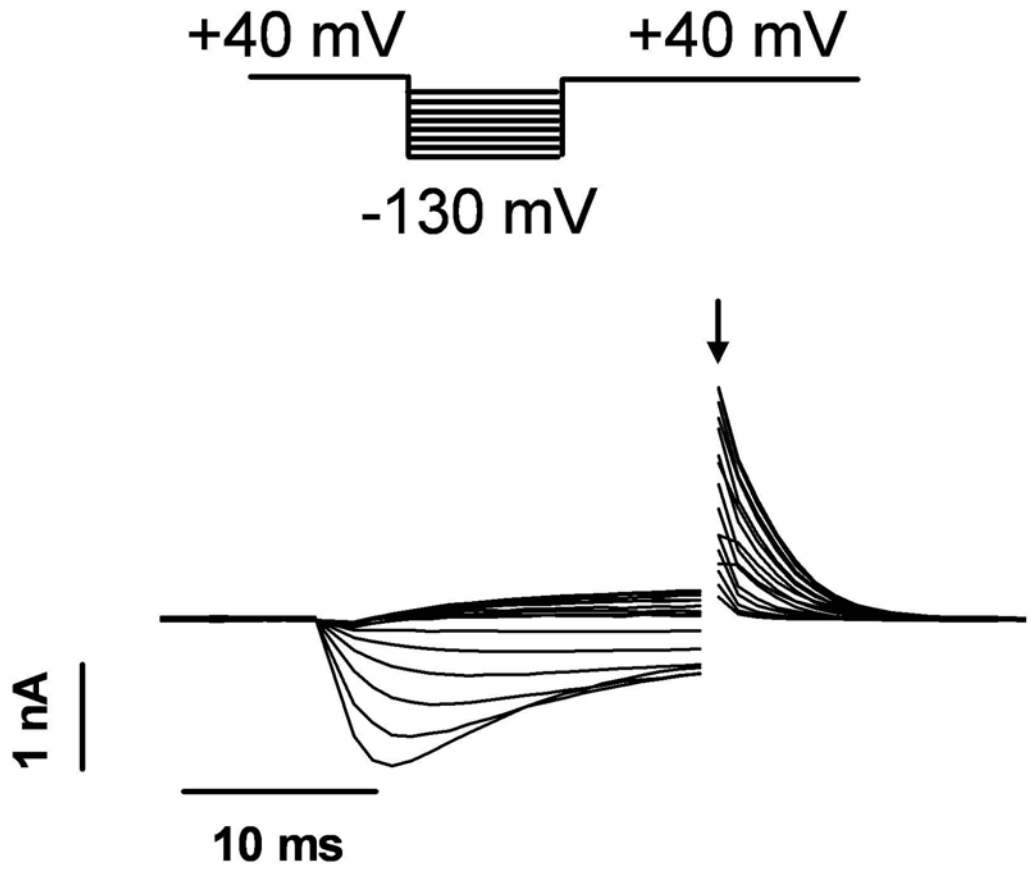

Online Figure I: Current records obtained with the protocol used to assess steady-state inactivation in cells expressing WT Kv11.1 channels. After inactivation was allowed to relax to steady-state at potentials ranging from -130 to +20 mV during 20 ms, membrane potential was stepped to +40 mV for 480 ms. The initial current on stepping to +40 mV (arrow) gave the relative number of open channels. Thus, inactivation curves were constructed by plotting the current amplitude at +40 mV as a function of the interpulse potential.

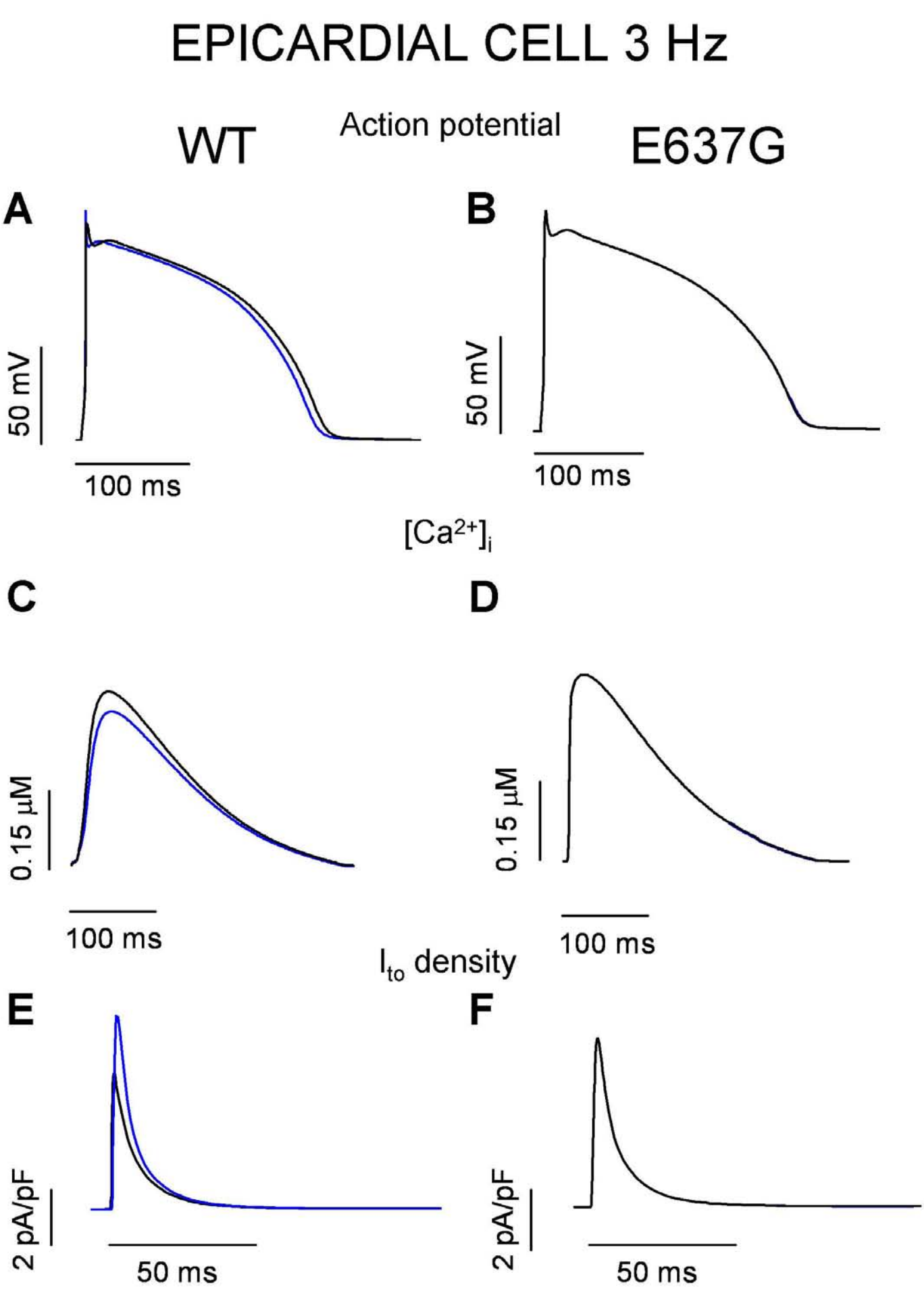

Online Figure II: (A,B) Superimposed traces of two consecutive epicardial action potentials obtained by running the Grandi-Bers model at 3 Hz under basal conditions (A) or when integrating all the I_{Kr} modifications induced by the p.E637G mutation (B). (C-F) Superimposed traces of $[Ca^{2+}]_i$ transients (C,D) and I_{to} (E,F) corresponding to the action potentials shown in A and B.